

AD-A269 864



## REPORT DOCUMENTATION PAGE

Form Approved  
OMB No. 0704-0188

(2)

Public reporting burden for this collection of information is estimated to average 1 hour per response, including the time for reviewing instructions, searching existing data sources, gathering and maintaining the data needed, and completing and reviewing the collection of information. Send comments regarding this burden estimate or any other aspect of this collection of information, including suggestions for reducing this burden, to Washington Headquarters Services, Directorate for Information Operations and Reports, 1215 Jefferson Davis Highway, Suite 1204, Arlington, VA 22202-4302, and to the Office of Management and Budget, Paperwork Reduction Project (0704-0188), Washington, DC 20503.

1. AGENCY USE ONLY (Leave blank)		2. REPORT DATE August 1993		3. REPORT TYPE AND DATES COVERED	
4. TITLE AND SUBTITLE Applications of the Method for Transducer Transient Suppression to Various Transducer Types				5. FUNDING NUMBERS PE - 62314N TA - RJ14-T21-OTO WU - DN880-326	
6. AUTHOR(S) J. C. Piquette					
7. PERFORMING ORGANIZATION NAME(S) AND ADDRESS(ES) NAVAL RESEARCH LABORATORY UNDERWATER SOUND REFERENCE DETACHMENT PO BOX 568337 ORLANDO, FL 32856-8337				8. PERFORMING ORGANIZATION REPORT NUMBER	
9. SPONSORING/MONITORING AGENCY NAME(S) AND ADDRESS(ES) OFFICE OF NAVAL RESAERCH 800 N. QUINCY STREET ARLINGTON VA 22217-5000				10. SPONSORING/MONITORING AGENCY REPORT NUMBER	
11. SUPPLEMENTARY NOTES					
12a. DISTRIBUTION/AVAILABILITY STATEMENT  Approved for public release; distribution unlimited.				12b. DISTRIBUTION CODE	
13. ABSTRACT (Maximum 200 words) Recently, a new method for suppressing the transient pressure radiation ordinarily produced by a projector in response to drive turnon and turnoff has been described [J. C. Piquette, "Method for transducer transient suppression I. Theory," J. Acoust. Soc. Am. <b>92</b> , 1203-1213 (1992) and "II. Experiment," J. acoust. Soc. Am. <b>92</b> , 1214-1221 (1992)]. The experiments described in the earlier reports involved application of the method primarily to piezoelectric spherical transducers, although one preliminary application to an array of piezoelectric tubes was also considered. The present work involved the application of the method to a variety of transducer types to which the method had not been applied previously. These types are (i) flexural disk, (ii) Helmholtz resonator, (iii) moving coil, (iv) inductor-tuned Tonpilz, and (v) a dual transducer array of piezoelectric squares and disks. A high degree of transient suppression was observed in all units that were tested. Equivalent circuits useful for designing the transient-suppressing drive are also provided.					
14. SUBJECT TERMS Transducer Transient Suppression Transducer Radiation Transducer Calibration Equivalent Circuits				15. NUMBER OF PAGES 6	
				16. PRICE CODE	
17. SECURITY CLASSIFICATION OF REPORT UNCLASSIFIED	18. SECURITY CLASSIFICATION OF THIS PAGE UNCLASSIFIED	19. SECURITY CLASSIFICATION OF ABSTRACT UNCLASSIFIED	20. LIMITATION OF ABSTRACT UL		

**Best  
Available  
Copy**

## GENERAL INSTRUCTIONS FOR COMPLETING SF 298

The Report Documentation Page (RDP) is used in announcing and cataloging reports. It is important that this information be consistent with the rest of the report, particularly the cover and title page. Instructions for filling in each block of the form follow. It is important to *stay within the lines* to meet optical scanning requirements.

**Block 1. Agency Use Only (Leave blank).**

**Block 2. Report Date.** Full publication date including day, month, and year, if available (e.g. 1 Jan 88). Must cite at least the year.

**Block 3. Type of Report and Dates Covered.** State whether report is interim, final, etc. If applicable, enter inclusive report dates (e.g. 10 Jun 87 - 30 Jun 88).

**Block 4. Title and Subtitle.** A title is taken from the part of the report that provides the most meaningful and complete information. When a report is prepared in more than one volume, repeat the primary title, add volume number, and include subtitle for the specific volume. On classified documents enter the title classification in parentheses.

**Block 5. Funding Numbers.** To include contract and grant numbers; may include program element number(s), project number(s), task number(s), and work unit number(s). Use the following labels:

C - Contract	PR - Project
G - Grant	TA - Task
PE - Program Element	WU - Work Unit Accession No.

**Block 6. Author(s).** Name(s) of person(s) responsible for writing the report, performing the research, or credited with the content of the report. If editor or compiler, this should follow the name(s).

**Block 7. Performing Organization Name(s) and Address(es).** Self-explanatory.

**Block 8. Performing Organization Report Number.** Enter the unique alphanumeric report number(s) assigned by the organization performing the report.

**Block 9. Sponsoring/Monitoring Agency Name(s) and Address(es).** Self-explanatory.

**Block 10. Sponsoring/Monitoring Agency Report Number. (If known)**

**Block 11. Supplementary Notes.** Enter information not included elsewhere such as: Prepared in cooperation with...; Trans. of...; To be published in... When a report is revised, include a statement whether the new report supersedes or supplements the older report.

**Block 12a. Distribution/Availability Statement.** Denotes public availability or limitations. Cite any availability to the public. Enter additional limitations or special markings in all capitals (e.g. NOFORN, REL, ITAR).

DOD - See DoDD 5230.24, "Distribution Statements on Technical Documents."

DOE - See authorities.

NASA - See Handbook NHB 2200.2.

NTIS - Leave blank.

**Block 12b. Distribution Code.**

DOD - Leave blank.

DOE - Enter DOE distribution categories from the Standard Distribution for Unclassified Scientific and Technical Reports.

NASA - Leave blank.

NTIS - Leave blank.

**Block 13. Abstract.** Include a brief (Maximum 200 words) factual summary of the most significant information contained in the report.

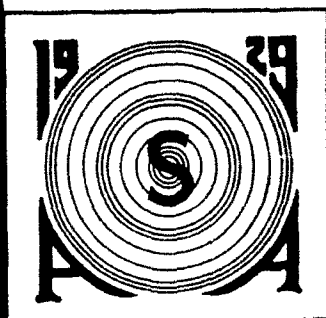
**Block 14. Subject Terms.** Keywords or phrases identifying major subjects in the report.

**Block 15. Number of Pages.** Enter the total number of pages.

**Block 16. Price Code.** Enter appropriate price code (NTIS only).

**Blocks 17. - 19. Security Classifications.** Self-explanatory. Enter U.S. Security Classification in accordance with U.S. Security Regulations (i.e., UNCLASSIFIED) If form contains classified information, stamp classification on the top and bottom of the page.

**Block 20. Limitation of Abstract.** This block must be completed to assign a limitation to the abstract. Enter either UL (unlimited) or SAR (same as report) An entry in this block is necessary if the abstract is to be limited. If blank, the abstract is assumed to be unlimited.



Reprinted from

# THE JOURNAL of the Acoustical Society of America

Vol. 94, No. 2, Pt. 1, August 1993

## Applications of the method for transducer transient suppression to various transducer types

Jean C. Piquette

Naval Research Laboratory, Underwater Sound Reference Detachment, P.O. Box 568337, Orlando,  
Florida 32856-8337

pp. 646-651

Accession For	
NTIS	CRA&I <input checked="" type="checkbox"/>
DTIC	TAB <input type="checkbox"/>
Unannounced	<input type="checkbox"/>
Justification	
By	
Distribution /	
Availability Codes	
Dist	Avail and/or Special
A-1	20

DTIC QUALITY INSPECTION 1

93-22167



# Applications of the method for transducer transient suppression to various transducer types

Jean C. Piquette

Naval Research Laboratory, Underwater Sound Reference Detachment, P.O. Box 568337, Orlando, Florida 32856-8337

(Received 5 October 1992; revised 29 January 1993; accepted 27 April 1993)

Recently, a new method for suppressing the transient pressure radiation ordinarily produced by a projector in response to drive turnon and turnoff has been described [J. C. Piquette, "Method for transducer transient suppression I. Theory," *J. Acoust. Soc. Am.* **92**, 1203–1213 (1992) and "II. Experiment," *J. Acoust. Soc. Am.* **92**, 1214–1221 (1992)]. The experiments described in the earlier reports involved application of the method primarily to piezoelectric spherical transducers, although one preliminary application to an array of piezoelectric tubes was also considered. The present work involved the application of the method to a variety of transducer types to which the method had not been applied previously. These types are (i) flexural disk, (ii) Helmholtz resonator, (iii) moving coil, (iv) inductor-tuned Tonpilz, and (v) a dual transducer array of piezoelectric squares and disks. A high degree of transient suppression was observed in all units that were tested. Equivalent circuits useful for designing the transient-suppressing drive are also provided.

TACS numbers: 43.85.Vb, 43.85.Wc, 43.20.Px

## INTRODUCTION

References 1 and 2 describe a new method for achieving suppression of the transient pressure radiation ordinarily produced when a transducer is stimulated with a gated-sine driving-voltage waveform. (The reader wishing to know why the solution of this problem is of interest, and wishing to see a summary of other work in this area, is directed to Ref. 1.) The method is based on preforming the drive. An equivalent circuit is required for the transducer that is to be driven in the transient-suppressed mode. The voltage waveform appearing across the electrical elements that represent radiation loading is taken to be a scaled replica of the pressure waveform radiated into the far field of the transducer. The driving-voltage waveform required to produce a transient-suppressed output is determined by assuming a perfect gated-sinusoidal voltage across the radiation-load elements, and then "calculating backward" through the circuit to the voltage source. Constants of integration that arise during the calculation are evaluated in such a way as to satisfy the initial conditions, i.e., the initial values of the circuit variables. During source turnon, the initial conditions enforce the requirements that charges and currents are zero. During source turnoff, the "initial" conditions enforce the requirements that charges and currents are continuous with respect to their values immediately prior to turnoff. If the number of integration constants that arise in the circuit calculations is equal to the number of initial conditions, the transient-suppression solution often is exact; otherwise, it is an approximation. (When the number of integration constants is unequal to the number of initial conditions, no exact analytical solution exists to the transient-suppression problem as posed in Ref. 1.) The interested reader is directed to Refs. 1 and 2 for a more detailed description of the method.

In the preliminary experimental work reported in Ref. 2, the method was applied to several piezoelectric spheres and to an array of piezoelectric tubes. The method was shown to be highly successful in suppressing transient radiation from the limited classes of transducer types that were tested. In the present paper, the results of applying the method to broader classes of transducer types are reported. These types are (i) flexural disk, (ii) Helmholtz resonator, (iii) moving coil, (iv) inductor-tuned Tonpilz, and (v) a dual transducer array of piezoelectric squares and disks.

## I. EQUIVALENT CIRCUITS

Figures 1–3 display the equivalent circuits that have been found to be useful in deducing the transient-suppressing driving-voltage waveforms for a variety of transducers. Figure 1 shows the equivalent circuit used in the previous work on the present method;<sup>1,2</sup> this circuit is based on a circuit presented in Ref. 3. Figure 2 is a modified version of the circuit of Fig. 1, including an extra external electrical capacitance  $C_{ab}$  and an external split tuning inductor with inductance legs  $L_1$  and  $L_2$ . Figure 3 is a modified version of an equivalent circuit for a moving-coil transducer,<sup>4</sup> in which the radiation-load electrical elements are replaced with an inductor and resistor wired in parallel, as is the case for the radiation load in the circuits presented in Figs. 1 and 2. It should be understood that this procedure is not as accurate as the analysis based on the circuits of Figs. 1 and 2, since magnetic circuits may contain nonlinear resistance components and the mobility analogy upon which the circuit of Fig. 3 is based requires a series capacitor and resistor radiation load for frequency-independent circuit elements. (Nonetheless, the circuit elements of Fig. 3, as well as those of Figs. 1 and 2, are taken

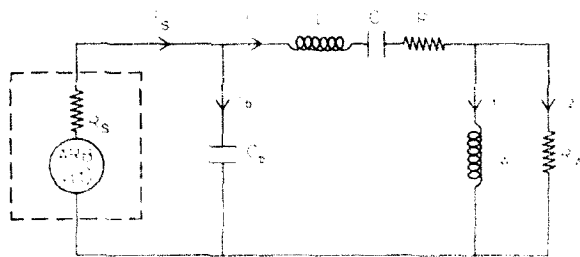


FIG. 1. Equivalent circuit originally derived for a spherical transducer,<sup>1</sup> but successfully applied to an array of piezoelectric tubes (see Ref. 2), a flexural disk, a Helmholtz resonator, and a dual array of piezoelectric disks and squares:  $C_b$ —blocked capacitance;  $L$ ,  $C$ ,  $R$ —motional inductance, capacitance, and resistance, respectively;  $L_u$ ,  $R_u$ —reactive and resistive components of radiation loading, respectively;  $i_1, i_2, i_3, i_4$ —currents. The symbol ARB denotes an arbitrary waveform generator of internal resistance  $R$ , producing the arbitrary voltage waveform  $V(t)$ .

to be frequency independent.) We choose to use this procedure since it results in some mathematical simplification and, as we shall see in Sec. II B, the method produces satisfactory results in the case to which it is applied here.<sup>5</sup>

Since the transient-suppression problem for the equivalent circuit of Fig. 1 is considered in detail in Ref. 1, further discussion of this case will be avoided here.

### A. Inductor-tuned Tonpilz circuit

The circuit of Fig. 2 is considered first. In what follows,  $\tau$  denotes the desired total duration of the radiated pulse, and is assumed to be equal to a whole number of half-cycles of the drive frequency. The symbol  $\omega_0$  denotes the angular drive frequency,  $t=0$  is the moment of source turnon,  $V_o$  is an arbitrarily selectable output-voltage amplitude [see Eq. (2) of Ref. 1],  $q$  is the charge on capacitor  $C$ , and  $q_b$  is the charge on capacitor  $C_b$ . By following the methodology outlined in the Introduction, the drive voltage for the turnon interval  $0 < t < \tau$  is found to be

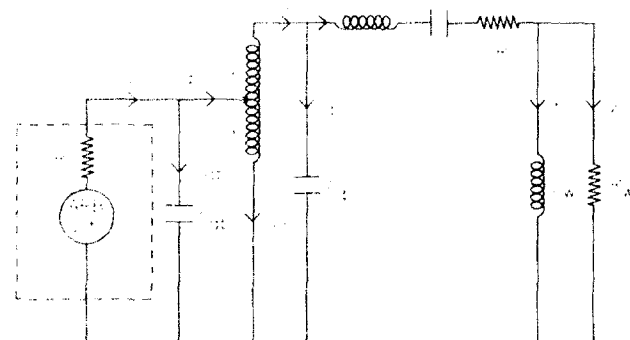


FIG. 2. Equivalent circuit for an inductor-tuned Tonpilz transducer. The elements  $L_1$ ,  $L_2$ , and  $C_{ab}$  are external electrical elements included to adjust transducer performance. The remaining elements are the same as in Fig. 1.

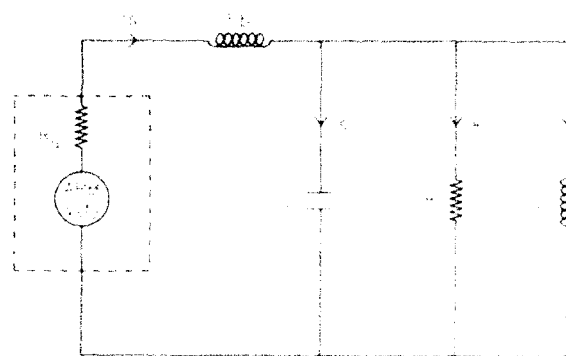


FIG. 3. Equivalent circuit for a moving-coil transducer, based on Ref. 4. The electromechanical transformers of Ref. 4 have been removed from the circuit in the manner of Ref. 3. The series combination of elements used in Ref. 4 to represent radiation loading has been replaced by a parallel combination of elements, also in the manner of Ref. 3. The elements  $L$  and  $R$  represent combinations of motional and radiative elements. The element  $C$  is the motional capacitance, and  $L_u$  is the blocked inductance. The remaining elements are as in Fig. 1. Nonlinear resistance effects are assumed to be small and intentionally omitted.

$$V(t) = i_1(t)R_s + L_2 \frac{di_{L_2}(t)}{dt} + L \frac{di(t)}{dt} + \frac{q(t)}{C} + i(t)R + V_o \sin(\omega_0 t) \quad (0 < t < \tau), \quad (1)$$

where the currents and charges are determined by writing and solving the usual loop and nodal equations. For example, the equation obtained for the circuit parameter  $i_{L_1}(t)$  is

$$i_{L_1}(t) = \frac{V_o t^2}{2L_u L_1 C \omega_0} + \frac{V_o t}{R_u C L_1 \omega_0} + \frac{V_o}{L_1 \omega_0} \left( 1 - \frac{1}{L_u C \omega_0^2} \right) \times [1 - \cos(\omega_0 t)] - \frac{V_o}{R_u C L_1 \omega_0^2} \sin(\omega_0 t) + \frac{L_2}{L_1} [i_{L_2}(t) - i_{L_2}(0)] + \frac{L}{L_1} i(t) + \frac{R}{L_1} q(t). \quad (2)$$

[The explicit sine and cosine terms of Eqs. (1) and (2) arise from the assumed output voltage. See Ref. 1.]

The drive voltage for the turnoff interval  $t \geq \tau$  depends upon whether an even or odd number of half-cycles is radiated. For the even-number half-cycle case, we find

$$V(t) = \frac{V_o R_s \tau}{C L_1 L_u \omega_0} (t - \tau) + i_{L_1}(\tau) R_s + \frac{V_o \tau}{L_u C \omega_0} \quad (t \geq \tau, \text{ even number of half-cycles}), \quad (3)$$

and for the odd-number half-cycle case we find

$$\begin{aligned}
V(t) = & \frac{V_o R_s}{C L_u \omega_0} (t^2 - \tau t) + \frac{2 V_o R_s}{\omega_0} \left( \frac{1}{R_u C} + \frac{R}{L_u} \right) (t - \tau) \\
& + i_{L_s}(\tau) R_s + \left( 1 + \frac{C_b}{C} \right) \frac{2 V_o R_s}{L_u \omega_0} + \frac{2 L_1 C_{ab} V_o R_s}{C L_u \omega_0} \\
& + \frac{V_o}{L_u C \omega_0} (2t - \tau) + \frac{2 V_o}{R_u C \omega_0} + \frac{2 V_o R}{L_u \omega_0} \\
& (t \geq \tau, \text{ odd number of half-cycles}). \quad (4)
\end{aligned}$$

It is interesting to note that in addition to the pedestal, ramp, and phase-shifted sinusoidal components that were found to be needed to drive the circuit of Fig. 1 in the transient-suppressed mode,<sup>1</sup> the circuit of Fig. 2 is found to also require a parabolic drive term [note Eq. (2)].

### B. Moving coil with parallel-element radiation load

Once again following the methodology outlined in the Introduction, we find by analyzing the circuit of Fig. 3 that the drive for the turnon interval is

$$V(t) = i_s(t) R_s + L_b \frac{di_s(t)}{dt} + V_o \sin(\omega_0 t) \quad (\tau > t > 0), \quad (5)$$

where

$$\begin{aligned}
i_s(t) = & C V_o \omega_0 \cos(\omega_0 t) + \frac{V_o}{R} \sin(\omega_0 t) \\
& + \frac{V_o}{L \omega_0} [1 - \cos(\omega_0 t)]. \quad (6)
\end{aligned}$$

As usual, the turnoff drive assumes different forms for the even-number and odd-number half-cycle output cases. For the even-number half-cycle case, we find

$$V(t) = 0 \quad (t \geq \tau, \text{ even number of half-cycles}). \quad (7)$$

For the odd-number half-cycle case, we find

$$V(t) = \frac{2 V_o R_s}{L \omega_0} \quad (t \geq \tau, \text{ odd number of half-cycles}). \quad (8)$$

## II. APPLICATIONS TO VARIOUS TRANSDUCER TYPES

### A. Numerical implementation

The method described in Refs. 1 and 2 requires that a high-order differential equation be solved in the general case. However, sinusoidal steady-state circuit analysis is often preferable to directly solving the differential equation, especially since modern computers perform Fourier transforms and their inverses quite efficiently. The circuit response to an arbitrary drive is deduced by first decomposing the drive into steady-state sinusoids via the discrete Fourier transform (DFT), multiplying each frequency component by the circuit transfer function, and then synthesizing the output waveform using the inverse DFT. This is precisely the approach that was used here to implement the

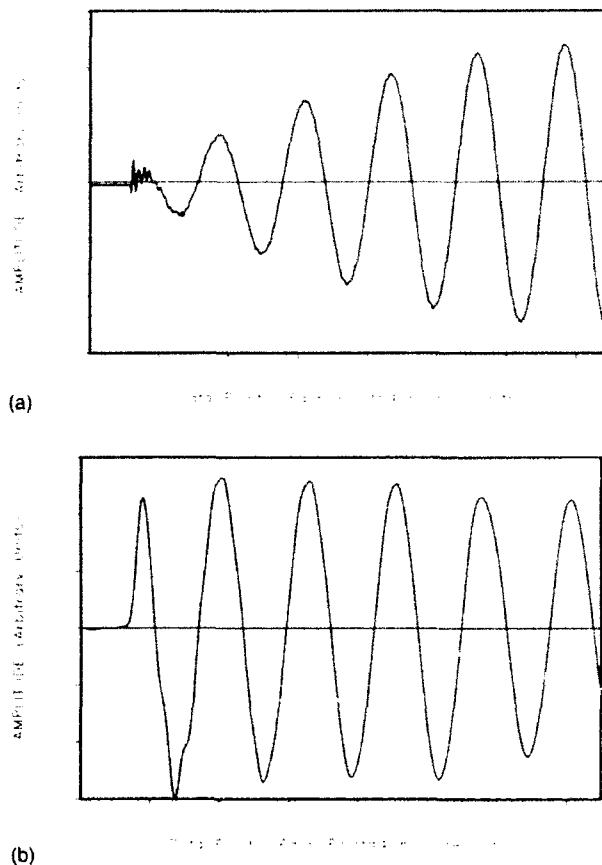


FIG. 4. Observed responses of the flexural disk transducer. Frequency is 1 kHz. Digitization rate used in data acquisition was 250 kHz. (a) gated-sine response; (b) transient-suppressed response. Steady-state behavior is seen after approximately 1 cycle. Arrival of facility reflections shortly after data point 1000 is evident. Waveform was acquired using an 80-dB-per-decade low-pass filter with its cutoff set at 5 kHz to inhibit observation of higher-order vibrational modes.

method described in Refs. 1 and 2 without the necessity of analytically solving the relevant high-order differential equation.

### B. Applications

The first example we examine is that of a flexural disk transducer with a  $Q$  of about 12 and a resonance frequency of about 1 kHz. This transducer has been studied previously<sup>6</sup> since its large  $Q$  and low resonance frequency makes accurate calibration of this device difficult to achieve in existing test facilities.

The response of this transducer to a 1-kHz gated-sine drive is shown in Fig. 4(a). This waveform was acquired in the Lake Facility of USRD, where approximately 4 ms of reflection-free data can be acquired. It is evident from Fig. 4(a) that the transducer has not achieved steady state by 4 ms and, in fact, this device would require about 12 ms to achieve steady state.

The transient suppression method was next applied to the transducer. Although the equivalent circuit of Fig. 1 was originally devised for a spherical transducer,<sup>1</sup> it was found in the present work to also be suitable for evaluating the flexural disk transducer. When driven at resonance us-

ing the transient-suppressing driving-voltage waveform derived from the equations of Ref. 1, the pressure waveform of Fig. 4(b) was produced. [In Fig. 4(a) and (b), as well as in subsequent figures, the arbitrary units used are consistent between each gated-sine and transient-suppressed waveform. Therefore, the reduction in amplitude due to driving in the transient-suppressed mode, as discussed in Ref. 2, is apparent.] The waveform displays reasonably steady-state behavior after about 1 cycle. Thus, the present method has effectively reduced the  $Q$  of the transducer from about 12 to about 1. Note also from Fig. 4(b) that the arrival of surface and bottom facility reflections (shortly after about data point number 1000) is evident, in contradistinction to Fig. 4(a). The difficulty in seeing the reflected arrivals in Fig. 4(a) can be understood from the fact that the gradual exponential turnon of the transducer in the gated-sine drive mode causes the reflections to blend smoothly with the directly radiated waveform, while the rapid turnon of the transient-suppressed waveform causes reflected arrivals to add to the direct radiation in an easily visible stair-step manner.

Another transducer for which the circuit of Fig. 1 was found to be suitable is the French JANUS<sup>7</sup> Helmholtz-resonator transducer. This transducer has two resonances, one at about 630 Hz and another at about 1080 Hz. In Fig. 5(a) is shown the response of the JANUS Helmholtz transducer to a 650-Hz gated-sine drive. This waveform was again acquired in the USRD Lake Facility, so data points after approximately data point 1000 are contaminated with surface and bottom facility reflections. Nonetheless, the high  $Q$  of the transducer is apparent. The response of the JANUS Helmholtz transducer to the transient-suppressing drive designed using the equivalent circuit of Fig. 1 is displayed in Fig. 5(b). The effects of higher-order modes are evident in the early portions of the waveform. Steady state appears to have been achieved after about 2 cycles. Although surface and bottom reflections are still expected at about data point number 1000, the influence of these reflections in this case appears to be relatively small.

We consider next a Tonpilz transducer. This transducer has additional external electrical elements, including a split tuning inductor. The behavior of this device is well described by the equivalent circuit of Fig. 2. The gated-sine response near resonance is shown in Fig. 6(a), and the transient-suppressed response based on the circuit of Fig. 2 is shown in Fig. 6(b). This transducer has a  $Q$  of about 8. As can be seen from Fig. 6(b), the present method has reduced the effective  $Q$  to about 2.5.

In Fig. 7(a) is shown the response of a J9 (moving-coil) transducer<sup>8</sup> to a gated-sine drive at 500 Hz. The corresponding transient-suppressed waveform, obtained by analyzing the circuit of Fig. 3, is shown in Fig. 7(b). [The 500-Hz frequency was selected for examination here because the response of the transducer at this frequency, displayed in Fig. 7(a), clearly exhibits the nonsinusoidal waveshape that characteristically results when a resonant transducer is driven with a gated sinusoid.] The negative-

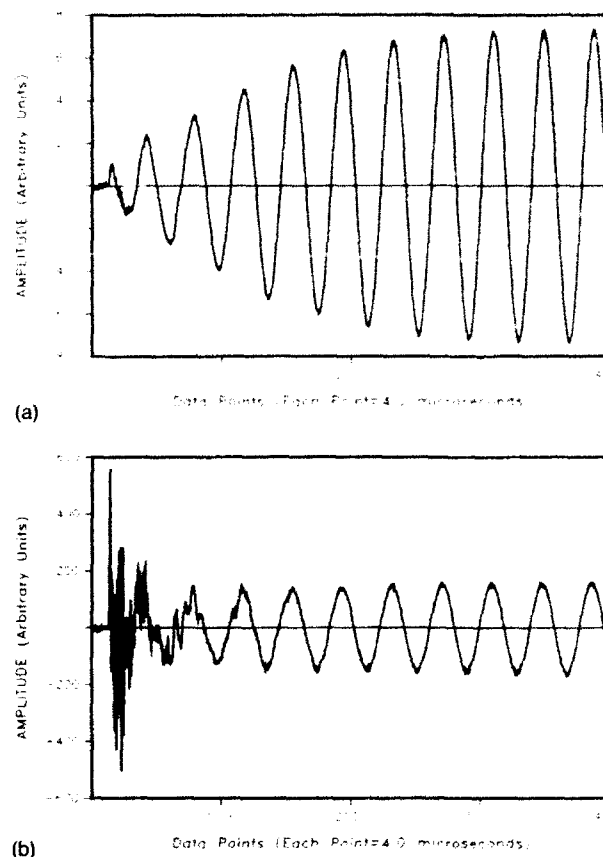


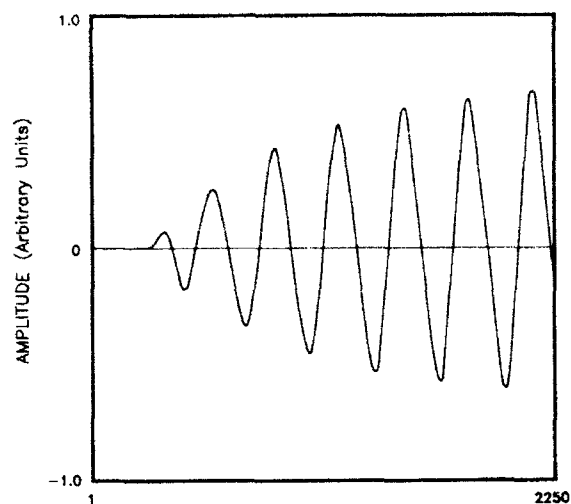
FIG. 5. Observed responses of the JANUS Helmholtz resonator. Data acquisition rate was 250 kHz: (a) response to a gated-sine drive of frequency 650 Hz; (b) response to the transient-suppressing drive of 650 Hz. No electrical filtering was used in data acquisition so the effects of the transducer's higher-mode resonances would be visible.

going signals appearing near the ends of Fig. 7(a) and (b) are surface reflections.

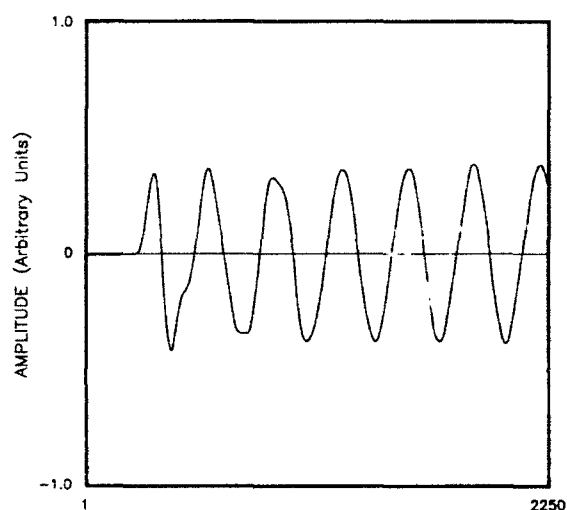
The final example considered here is the F33 transducer.<sup>8</sup> This case is of interest because it has been considered previously as the object of a transient-suppression study.<sup>9</sup> (The desired Hanning-windowed sinusoidal output waveforms considered in Ref. 9, however, exhibit much more gradual turnon and turnoff characteristics than the desired gated-sine output waveforms considered here, and thus exhibit significantly narrower bandwidth. The method of Ref. 9 utilized an inverse transfer-function approach to determine the required driving-voltage waveform. Inverse transfer-function methods encounter difficulties at zeros of the transfer function. The introduction of additional *ad hoc* functions into the transfer function was thus found in Ref. 9 to be necessary to successfully model the low-frequency behavior of the F33. The present method on the other hand, required only an analysis of the circuit of Fig. 1 to determine the required waveshape of the driving-voltage waveform.)

The F33 is a dual array of piezoelectric elements, designed to cover a relatively broad frequency band of 1–50 kHz when both arrays are driven simultaneously. In Fig. 8(a) is displayed the response of the F33 to a 4-cycle 10-kHz gated-sine driving-voltage waveform, while Fig. 8(b)





(a) DATA POINTS (EACH POINT=1 MICROSECOND)



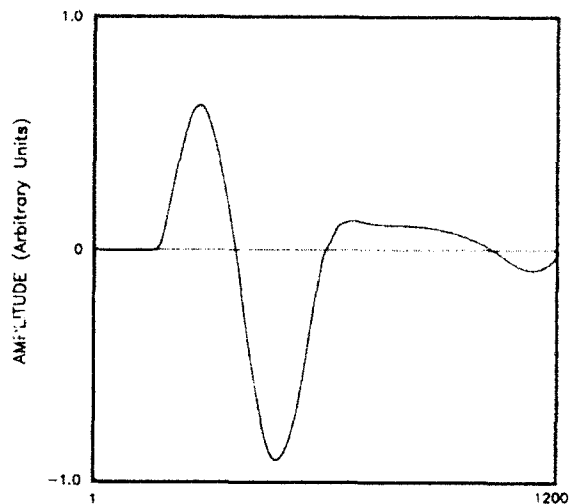
(b) DATA POINTS (EACH POINT=1 MICROSECOND)

FIG. 6. Observed responses of an inductor-tuned Tonpilz transducer. An 80-dB-per decade low-pass filter with its cutoff set approximately  $1\frac{3}{4}$  octaves above the drive frequency was used in data acquisition to inhibit observation of the effects of higher-mode resonances. Data acquisition rate was 1 MHz: (a) gated-sine response; (b) transient-suppressed response.

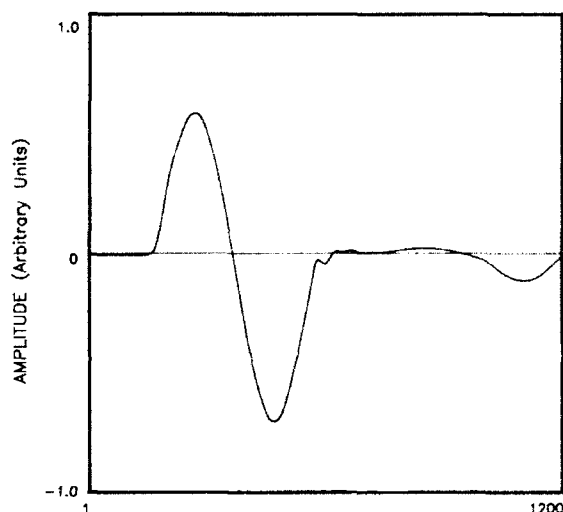
shows the corresponding transient-suppressed response. The signal appearing at the right side of Fig. 8(b) is not the result of a facility reflection as might be suspected. Rather, it is a ringdown that occurs when the pedestal component of the transient-suppressing drive that is applied during the turnoff interval is released. (See Fig. 4 of Ref. 1.) The appearance of this ringdown can be delayed arbitrarily by sufficiently lengthening the duration of the turnoff pedestal.

### III. SUMMARY, DISCUSSION, AND CONCLUSIONS

Applications of the transducer transient suppression method, originally described in Refs. 1 and 2, to broad classes of transducers to which the method had not been applied previously have been described. The transducer



(a) DATA POINTS (EACH POINT=5 MICROSECONDS)



(b) DATA POINTS (EACH POINT=5 MICROSECONDS)

FIG. 7. Observed responses of the J9 transducer. Data acquisition rate was 500 kHz: (a) gated-sine response; (b) transient suppressed response.

types to which the method has been newly applied are (i) flexural disk, (ii) Helmholtz resonator, (iii) inductor-tuned Tonpilz, (iv) moving coil, and (v) a dual array of piezoelectric disks and squares. A high degree of transient suppression was observed in all units that were tested.

It has been found that the simple equivalent circuit considered in Ref. 1 is unusually effective (and perhaps unreasonably effective) in designing the driving-voltage waveform required to reduce turnon and turnoff transient pressure radiation from a projector. This simple circuit was shown here to be effective in reducing transient radiation from the flexural disk, JANUS Helmholtz, and the dual piezoelectric element array. These three transducer types are additional examples beyond the three piezoelectric spheres and the array of piezoelectric tubes that were shown in Ref. 2 to have their transient radiation effectively suppressed by using a waveform deduced by analyzing the circuit of Fig. 1. Only a relatively minor modification of

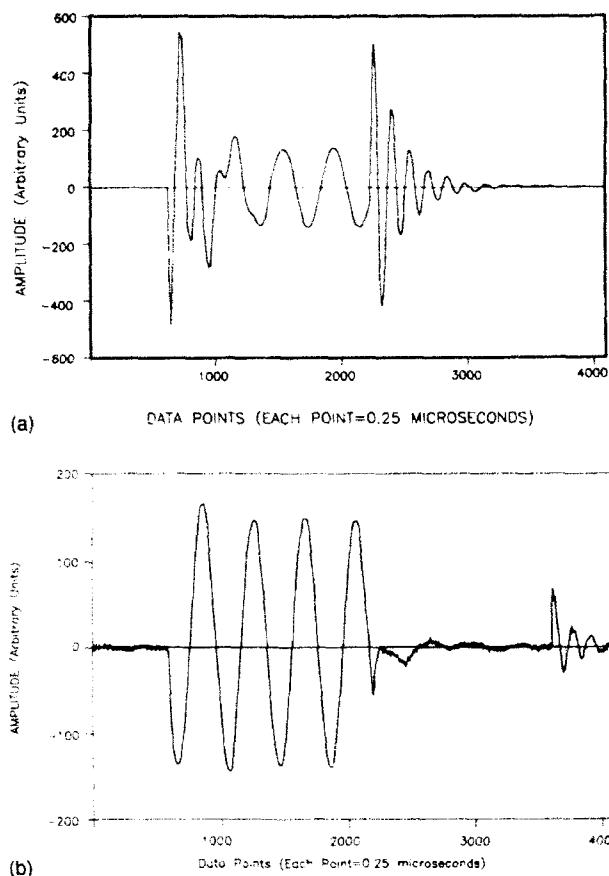


FIG. 8. Observed responses of the F33 transducer. Frequency—10 kHz. Data acquisition rate was 4 MHz: (a) gated-sine response; (b) transient-suppressed response.

this original circuit was required to account for the influence of the additional external electrical elements included with the Tonpilz transducer that was studied (see Fig. 2). Why the simple circuit of Fig. 1 should be so effective in deriving the transient-suppressing waveform, even when it is applied to transducer types that are so different from the piezoelectric sphere for which it was originally developed, is unknown.<sup>10</sup>

Future research in this area includes developing a computer-disk library of equivalent circuit element values to permit transient-suppressed operation of a wide variety of standard transducers.<sup>9</sup> The success of the present research suggests that only the three equivalent circuits of Figs. 1–3 may be required to drive any of the transducers of Ref. 8 in the transient-suppressed mode. Other research

concerns the modification of the transient-suppressing waveform in a way that would permit easier electronic implementation than the present waveshapes (which include troublesome pedestal, ramp, and parabolic components). Applications of the method to transducer calibration and to reflection and scattering measurements are also anticipated.

## ACKNOWLEDGMENTS

I am indebted to A. C. Tims for suggesting the use of the equivalent circuit of Fig. 2 for analyzing the inductor-tuned Tonpilz transducer. I am also indebted to A. R. Garceau for his help in data acquisition. The JANUS Helmholtz transducer was provided by Dr. C. Giangreco of the Centre d' Etudes et de Recherches de Detection Sous-Marine, Le Brusc, France. This work was supported by the Office of Naval Technology.

<sup>1</sup>J. C. Piquette, "Method for transducer transient suppression I. Theory," *J. Acoust. Soc. Am.* **92**, 1203–1213 (1992).

<sup>2</sup>J. C. Piquette, "Method for transducer transient suppression II. Experiment," *J. Acoust. Soc. Am.* **92**, 1214–1221 (1992).

<sup>3</sup>A. C. Tims, T. A. Henriquez, and J. G. Williams, "A Transducer for Bottom-Scattering Measurements," NRL Memorandum Report 5616 (Dec. 1985).

<sup>4</sup>L. L. Beranek, *Acoustics* (McGraw-Hill, New York, 1954), p. 81, Fig. 3.43.

<sup>5</sup>The simplified circuit of Fig. 3 can also be justified theoretically in the following way: If the radiation load of the circuit of Ref. 4 is primarily resistive, the radiation resistance can be lumped with the mechanical resistance and the radiation reactance can be ignored. Although the far-field pressure waveform in the mobility analogy is proportional to the radiation-load current, when the radiation load is primarily resistive, the far-field pressure is also proportional to the radiation-load voltage, by virtue of Ohm's law. Hence, the voltage across resistor  $R$  of Fig. 3 can be used to determine the transient-suppressing drive voltage in an approximate way, and this approximation has been found to be successful in driving the J9 transducer.<sup>6</sup>

<sup>6</sup>J. D. George and P. L. Ainsleigh, "A Signal Model for Transducer Calibration in Multipath Environments," in *Proceedings of the Third International Workshop on Transducers for Sonics and Ultrasonics* (Technomic Publishing Co., Lancaster, PA, 1993), pp. 369–371.

<sup>7</sup>D. Boucher, "New Solutions of Low Frequency Sonar Projectors," in *Proceedings of the Third International Workshop on Transducers for Sonics and Ultrasonics* (Technomic Publishing Co., Lancaster, PA, 1993), pp. 17–37.

<sup>8</sup>L. E. Ivey, *USRD Transducer Catalog* (Naval Research Laboratory, Orlando, FL, 1992).

<sup>9</sup>A. K. Walden, "Signal processing techniques on an underwater acoustic projector," Master's thesis, Georgia Institute of Technology (1991).

<sup>10</sup>It might be supposed that this unreasonable effectiveness is attributable to the fact that the low-frequency behavior of many transducers is similar. However, this fails to explain how transients associated with higher-mode resonances, such as those that are apparent in the F43 transducer considered in Ref. 2, and the F33 considered here, are suppressed.